J Neurophysiol 94: 3826–3835, 2005.
First published August 24, 2005; doi:10.1152/jn.00601.2005.

Early Appearance of Inhibitory Input to the MNTB Supports Binaural Processing During Development

Joshua S. Green[1] and Dan H. Sanes[1,2]
[1]*Center for Neural Science and* [2]*Department of Biology, New York University, New York, New York*

Submitted 10 June 2005; accepted in final form 22 August 2005

Green, Joshua S. and Dan H. Sanes. Early appearance of inhibitory input to the MNTB supports binaural processing during development. *J Neurophysiol* 94: 3826–3835, 2005. First published August 24, 2005; doi:10.1152/jn.00601.2005. Despite the peripheral and central immaturities that limit auditory processing in juvenile animals, they are able to lateralize sounds using binaural cues. This study explores a central mechanism that may compensate for these limitations during development. Interaural time and level difference processing by neurons in the superior olivary complex depends on synaptic inhibition from the medial nucleus of the trapezoid body (MNTB), a group of inhibitory neurons that is activated by contralateral sound stimuli. In this study, we examined the maturation of coding properties of MNTB neurons and found that they receive an inhibitory influence from the ipsilateral ear that is modified during the course of postnatal development. Single neuron recordings were obtained from the MNTB in juvenile (postnatal day 15–19) and adult gerbils. Approximately 50% of all recorded MNTB neurons were inhibited by ipsilateral sound stimuli, but juvenile neurons displayed a much greater suppression of firing as compared with those in adults. A comparison of the prepotential and postsynaptic action potential indicated that inhibition occurred at the presynaptic level, likely within the cochlear nucleus. A simple linear model of level difference detection by lateral superior olivary neurons that receive input from MNTB suggested that inhibition of the MNTB may expand the response of LSO neurons to physiologically realistic level differences, particularly in juvenile animals, at a time when these cues are reduced.

INTRODUCTION

The superior olivary complex (SOC) is generally considered to be the site at which binaural localization cues are first processed in the mammalian central auditory system. This view is supported by electrophysiological recordings that show SOC discharge rates varying systematically with interaural level (ILD) or time differences (ITD) (Boudreau and Tsuchitani 1968; Goldberg and Brown 1969; Spitzer and Semple 1995; Yin and Chan 1990). Furthermore, lesions of the SOC impair sound localization capabilities, suggesting that binaural computations in this area are necessary for spatial perceptual tasks (Kavanagh and Kelly 1992; Masterton et al. 1967). According to the simplest models of ILD and ITD processing, monaurally activated afferents converge at the lateral or medial superior olivary nuclei (LSO or MSO), where they are integrated by postsynaptic neurons. However, the monaural projections to SOC include an assortment of excitatory and inhibitory afferents (Grothe and Sanes 1993; Kil et al. 1995; Kuwabara and Zook 1992; Wu and Kelly 1994). Furthermore, there is growing recognition that many ventral cochlear nucleus neurons themselves receive a binaural input (Cant and Gaston 1982; Needham and Paolini 2003; Schofield and Cant 1996a,b; Shore et al. 1992, 2003).

The elaborate connectivity of SOC binaural circuits is of particular interest during postnatal development when axonal and dendritic arbors are remodeled (Henkel and Brunso-Bechtold 1991; Kapfer et al. 2002; Kil et al. 1995; Kim and Kandler 2003; Rietzel and Friauf 1998; Russell and Moore 1995; Sanes and Siverls 1991; Sanes et al. 1992). These connections also display alterations in neurotransmitter-receptor phenotype synaptic transmission, and intrinsic membrane properties (Joshi and Wang 2002; Kandler and Friauf 1995a,b; Kim and Kandler 2003; Korada and Schwartz 1999; Kotak et al. 1998; Sanes 1993; Svirskis et al. 2004). Together, these structural and functional changes may lead to qualitative differences in auditory coding properties. For example, juvenile LSO neurons display broader frequency tuning and encode a smaller range of ILDs as compared with those in adult animals (Sanes and Rubel 1988).

Coding properties are also influenced heavily by the pinnae and head size. In the juvenile ferret, auditory cortex neurons can display adult-like spatial coding properties when activated with dichotic stimuli that reflect the filtering characteristic of adult external ears (Mrsic-Flogel et al. 2003). Despite these peripheral and central constraints on auditory processing, developing animals can localize sounds using binaural cues (Kelly and Potash 1986). This raises the possibility that the developing nervous system makes use of age-specific specializations that improve perceptual discrimination given the physical limitations of the organism. Age-specific specializations are common in species that undergo metamorphosis, but they have not been explored in mammals.

The maturation of auditory coding properties was examined in the medial nucleus of the trapezoid body (MNTB), neurons that are activated by a single excitatory synapse from the contralateral cochlear nucleus called the calyx of Held (Friauf and Ostwald 1988; Galambos et al. 1959; Goldberg and Brown 1968; Guinan and Li 1990; Guinan et al. 1972; Held 1893; Kuwabara et al. 1991; Morest 1968; Smith et al. 1998; Sommer et al. 1993). MNTB neurons are also inhibited by contralateral tones outside of the conventional frequency response area (Kopp-Scheinpflug et al. 2003). In the present study, we found that 50% of MNTB neurons were binaurally influenced, and this effect was much stronger in juvenile animals, suggesting a developmental mechanism that could facilitate ILD coding.

Address for reprint requests and other correspondence: **Correspondence**: Dan H. Sanes, Center for Neural Science, 4 Washington Place, New York University, New York, NY 10003, Office 212-998-3924, FAX 212-995-4348, Email sanes@cns.nyu.edu

METHODS

Surgery

All protocols were reviewed and approved by the New York University Institutional Animal Care and Use Committee. Gerbils (*Meriones unguicalatus*) at postnatal day (P) 15–19 and adults were anesthetized with chloral hydrate (350 mg/kg) and ketamine (15 mg/kg). Surgical anesthesia was maintained with chloral hydrate (at least P19) or chloral hydrate and ketamine (adults) as described previously (Sanes and Rubel 1988). Supplements were given as indicated by a withdrawal response to toe pinch. Atropine (0.08 mg/kg) was given with initial anesthesia to minimize pulmonary secretions, and tracheotomies were performed on all animals. Core body temperature was monitored with a rectal probe and maintained at 37°C with a homeothermic blanket (Harvard Apparatus, Kent, UK). For stable recordings, the skull was glued to a head post, and the head and torso were raised so that the torso would not move against a surface during breathing. The pinnae were removed, and the tympanic annuli were exposed. The nervous system was accessed by making a dorsal midline incision, removing the external neck muscles, and transecting the dura mater underneath the foramen magnum.

Electrophysiology and sound delivery

All stimuli were delivered under closed-field calibrated conditions in a double-walled sound attenuated chamber (Industrial Acoustics) as described previously (Sanes et al. 1998). Speculae for sound delivery were placed close to the tympanic membrane and agar was applied to create a reliable seal. Glass electrodes containing 5–10% tetramethylrhodamine or fluorescein dextrans (3,000 MW, Molecular Probes, OR) in 2 M NaCl, or 2 M NaCl without dye, were lowered into the brain stem. Neural signals were amplified, filtered, and monitored on an oscilloscope and loudspeaker. A MALab system (Kaiser instruments, Irvine, CA) was used for stimulus generation, discrimination of unit activity, and data acquisition. During simultaneous acquisitions of pre- and postsynaptic action potentials, an oscilloscope (Yokogawa DL1540C) was used to trigger the MALab system off the postsynaptic action potentials, and MALab was used directly to discriminate the prepotentials. Stimulus delivery was calibrated for SPL relative to 20 μPa before each experiment with a condenser microphone (Brüel and Kjaer).

Response characterization

After isolation, each single unit was characterized for frequency tuning and for the presence of ipsilateral inhibition (50-ms tone pips, 2-s intertrial intervals, 5 trials for frequency tuning, 10 trials for rate-intensity functions). The 2-s intertrial interval was used to avoid response adaptation (Sanes and Constantine-Paton 1985). Sound-evoked responses were taken as spike counts obtained during the stimulus presentations. The best frequency (BF) is that which evokes the greatest discharge rate at a single intensity. Excitatory rate-intensity functions were obtained by presenting contralateral tones at increasing intensity levels. Excitatory thresholds were derived from visual inspection of these data. To confirm that these visual judgments were accurate, 10 rate-intensity functions were selected at random and processed with a MATLAB algorithm that searched for the first intensity at which the mean of the distribution of firing rates was significantly greater ($P < 0.05$, 1-tailed Student's t-test) than that of the distribution obtained over all lower intensities. An additional requirement was that the two subsequent data points also met the same criterion. In 9 of 10 instances, the algorithm agreed with our visual judgments; this success rate was considered sufficient to support the visual procedure.

To obtain inhibitory rate-level functions, a suprathreshold contralateral tone was delivered to evoke a baseline discharge rate, and ipsilateral tones were delivered concurrently at increasing intensities. The presence of inhibition was inferred visually by a decrease in spike rates associated with increasing ipsilateral intensities; the inhibitory threshold was the intensity level at which the decrease was first observed. To increase confidence in our assessments of inhibitory threshold, we again evaluated 10 functions at random using a MATLAB algorithm. In 9 of 10 cases tested, algorithmic and visual judgments were in agreement; as before, this result was considered adequate validation of the visual method.

One measure of the robustness of inhibition was the threshold difference between the two ears. A second method of quantifying inhibition involved presenting stimuli of increasing average binaural level at zero ILD, a physiologic ILD corresponding to a midline stimulus location. This procedure was used only when the presence of inhibition was established with an inhibitory rate-intensity function. To assess the influence of ipsilateral inhibition, the contralateral stimuli were repeated in the absence of ipsilateral sound. The strength of inhibition was computed by dividing the area between the binaural curve at 0 ILD and the corresponding monaural curve by the total area under the monaural curve (see Fig. 7*A*). To test whether the inhibition was significantly greater than random changes in discharge rate, monaural and binaural data were randomly reshuffled and the distribution of inhibition strengths expected by chance was derived from repeated reshuffling (MATLAB). For each of 110 observed inhibitory strengths, the probability of having obtained the result by chance was calculated by comparing the result with a distribution of inhibitory strengths derived from 2,000 pairs of simulated monaural and binaural curves. Cases in which P was calculated to be >0.05 were considered not to have inhibition at the physiologic ILDs and were assigned an inhibitory strength of 0.

In four cells, the MALAB system was set to separately count pre- and postsynaptic components so that the effects of inhibition on each component could be observed. These prepotentials and postsynaptic action potentials are readily distinguished in recordings from MNTB principal cells (Guinan and Li 1990). In the cases presented here, the largest component of the postsynaptic waveform and the prepotential had opposite polarities and could thus be segregated by simple adjustment of separate trigger thresholds. The recordings consisted of 25 trials; 500-ms contralateral and 100-ms ipsilateral tones were used.

Recording site verification

Most recordings were localized to the MNTB by a reliable electrophysiological criterion, the presence of a prepotential (Guinan and Li 1990). On occasion, fluorescent dye (see preceding text) was iontophoresed by passing anodal current (10 μA) for ~30 min to mark the recording site. After experiments, animals injected with dye were perfused with 4% paraformaldehyde, and the brains were post fixed for $\geq$24 h. Fixed brains were cut at 80 μm on a freezing microtome. Sections were viewed with a fluorescence microscope equipped with fluorescein and rhodamine-exciting filters. In all cases in which cells had a prepotential and were marked ($n = 8$), the dye was found within the MNTB. Recording sites that were within 20 μm of the marked site, or that were recorded between other cells localized to the MNTB, were also considered to be within the nucleus ($n = 3$ adult neurons, $n = 2$ juvenile neurons). All recordings presented here are from neurons confirmed to be in the MNTB by the above physiological and/or histological criteria. Examples of prepotentials and of an injection site are shown in Fig. 1.

Model of LSO responses

LSO responses at BF were modeled by adding the responses of simulated monaural inputs. These inputs included the ipsilateral anteroventral cochlear nucleus (AVCN), the ipsilateral MNTB, and the crossed AVCN pathway (a possible locus of inhibition of the MNTB). To evaluate the effect of inhibition of the MNTB, LSO responses were generated with and without ipsilateral inhibition to the MNTB.

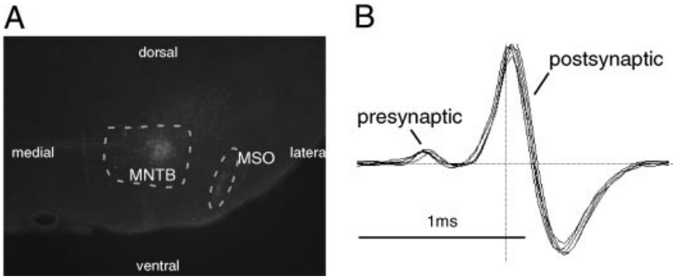

FIG. 1. An illustration of the methods used to localize units to the medial nucleus of the trapezoid body (MNTB). *A*: a rhodamine dextran injection site in the lateral portion of the rostral MNTB. - - -, approximate boundaries of the MNTB and medial superior olivary nucleus (MSO). The filled fibers exiting the MNTB medially are presumably retrogradely filled afferents from the contralateral VCN. *B*: extracellularly recorded waveforms from 1 of the units in the study. An early component corresponds to the presynaptic action potential (prepotential) and a larger, late component corresponds to the postsynaptic action potential (postpotential). The presence of a prepotential was considered confirmation that the unit was in the MNTB.

Michaelis-Menten equations were used to model inputs; the form of the equations was, $R = (I{*}R_{max})/(K_m + I)$ where R is the response at the input nucleus, I is the intensity level re threshold, R_{max} is the maximum firing rate, and K_m is a constant re threshold that sets the intensity level at which the response is half the maximal value. This equation was chosen for its monotonicity and for having parameters that relate to saturation and dynamic range. Values were chosen to approximate the conditions obtaining for juvenile animals. In particular, the thresholds, maximum firing rates and dynamic ranges (i.e., the K_m value) of the ipsilateral AVCN and the ipsilateral MNTB were set equal in accord with earlier observations in the LSO (Sanes and Rubel 1988). The crossed AVCN threshold was set to 15 dB higher than the thresholds for the other inputs because 15 dB was the median threshold difference between excitatory and inhibitory thresholds in the MNTB. The K_m value of the crossed AVCN pathway was set such that the dynamic range would be 93% of that of the other inputs; this was the average value obtained when the dynamic ranges of ipsilateral inhibition and contralateral excitation in the MNTB were compared (data not shown). R_{max} for the crossed pathway was set to half of that for the other nuclei, resulting in an inhibition strength near the median value for juvenile animals (inhibition strength = 0.24; median inhibition strength = 0.26). The spontaneous discharge rate of the LSO was set to 5 spikes/s (Sanes and Rubel 1988) by adding 5 spikes/s to all values in the response curve of the ipsilateral AVCN. All parameter settings are summarized in Table 1. The ranges of physiologic ILDs were derived from unpublished data (Green, Semple, and Sanes). In the case of the theoretical LSO response surfaces in Fig. 8, the chosen range was 5 dB, corresponding to the appropriate range at 3–5 kHz.

RESULTS

Single-unit recordings were obtained from 231 adult and 100 juvenile neurons. Contralateral rate-level functions were obtained, and poststimulus time histograms (PSTHs) were examined at 20–25 dB above threshold (Fig. 2). The PSTHs were all primary like (n = 61 adult, n = 42 juvenile). The first-spike latencies were obtained from these PSTHs using visual criteria and were found to be shorter in neurons from adult animals [adult: 6.1 ± 0.8 (SD) ms, n = 61; juvenile: 7.7 ± 1.4 ms, n = 38]. The latency differences between the age groups was significant ($P < 0.0001$, 2-tailed Student's t-test), and the respective distributions are shown in Fig. 2*B*. When rate-level functions reached a clear plateau, the 15–85% dynamic ranges of contralateral excitation were computed (Fig. 3*A*). The distribution of dynamic range values are plotted in Fig. 3*B*. The mean value for adult neurons was 24 ± 7 dB (n = 48) and for juvenile neurons was 19 ± 6 dB (n = 36). The difference was significant (P = 0.002, 2-tailed Student's t-test).

TABLE 1. *LSO model parameters*

Nucleus	Threshold, dB	R_{max}, spikes/s	K_m
Ipsi AVCN	55	80	10
Ipsi MNTB (excitation)	55	80	10
Crossed AVCN	70	40	18.9

The table indicates the parameters for the activation curves of each nucleus that determines the lateral superior olivary nucleus (LSO) output. The parameters are employed in Michaelis-Menten equations, as described in METHODS.

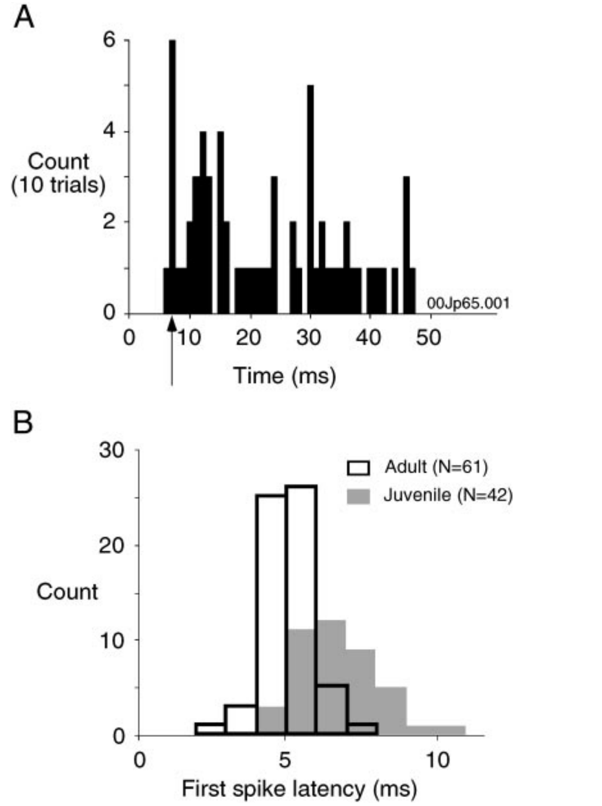

FIG. 2. *A*: a representative poststimulus time histogram (PSTH), in this case from an adult neuron, exhibits a primary-like discharge pattern at 25 dB above threshold (● in rate-intensity function plotted in Fig. 3*A*). The absence of a notch may be due to insufficient trials. Bin width is 1 ms. ↑, 1st-spike latency. *B*: distribution of 1st-spike latencies for both age groups shows that latency significantly shorter for adult neurons than those in juvenile animals.

Of 231 adult units 116 displayed inhibition at the BF (n = 46 animals). In neurons from juvenile animals 49 of 88 recorded neurons displayed inhibition (the determination of the proportion of inhibited cells excluded 12 MNTB neurons that were isolated during a deliberate search for inhibited neurons; n = 43 animals). The difference in proportion of inhibited cells between the age groups was not significant (P = 0.38, χ^2 analysis). The latency of excitation and inhibition were similar to one another, as shown in Fig. 4*A*. In four neurons examined, the inhibitory latency was 0, 2, 2, and 4 ms longer than the excitatory latency. An example of a cell that was responsive to ipsilateral sound, and a cell that was not responsive, are shown in Fig. 4*B*. To assess whether inhibition was observed only in

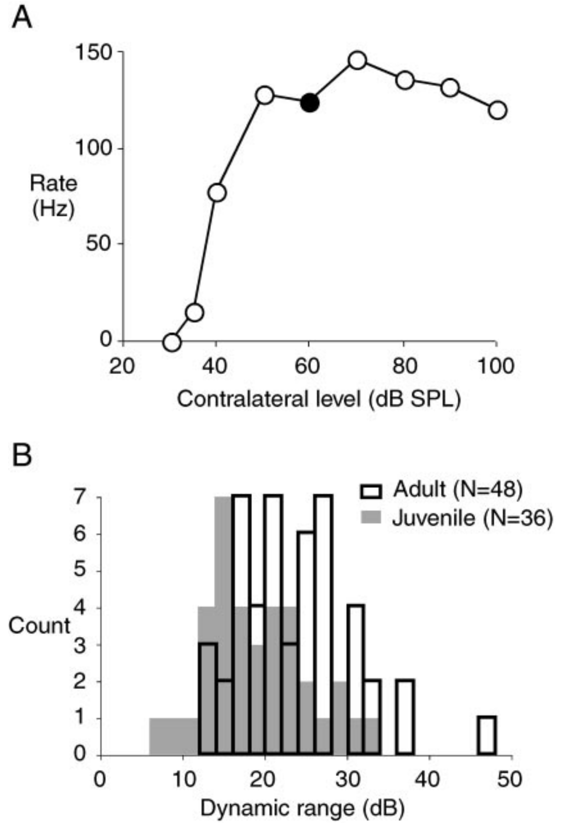

FIG. 3. *A*: rate-intensity function for contralateral excitation. The PSTH for the ● is shown in Fig. 2*A*. *B*: 15–85% dynamic range of the rate intensity functions are plotted for both age groups. The mean dynamic range was significantly smaller in juvenile animals.

some animals, perhaps due to the anesthetic state, we computed the proportions of cells inhibited within each animal for cases in which there were two or more recorded cells studied (Fig. 4*C*). A lack of clustering at the highest and lowest values indicated that inhibition did not appear to be restricted to a particular group of animals; within animals, cells were often heterogeneous with respect to ipsilateral inhibition. In some cases, it was possible to demonstrate that stronger excitatory drive could obscure the ipsilaterally evoked inhibition that was observed with lower contralateral sound levels, as shown in Fig. 4*D*.

To determine whether inhibition was operating at the MNTB neuron itself, we monitored the extracellularly recorded prepotential and postsynaptic action potential (Guinan and Li 1990). Using this approach, the effect of inhibition on both components was obtained in four adult cells. As shown in Fig. 5, prepotential and postsynaptic action potential activity were nearly identical before, during, and after the inhibition evoked by ipsilateral sound stimulation. This result was interpreted to mean that inhibition operates outside of the MNTB, perhaps at its cochlear nucleus afferent neurons via a crossed projection.

The robustness of ipsilateral inhibition was characterized in two ways. First, the excitatory and inhibitory thresholds were compared ($n = 61$ adult, $n = 41$ juvenile). Figure 6*A* illustrates the method by which the threshold differences were derived. Threshold differences spanned a wide range in both age groups, ranging from -15 to 60 dB in juvenile animals and from -15 to 80 dB in adults (Fig. 6*B*). There were no significant differences between the mean threshold difference in neurons from juvenile versus adult animals ($P = 0.35$, Student's *t*-test).

In a second set of measurements, the strength of inhibition was determined at zero ILD, corresponding to a midline stimulus location (Fig. 7*A*). To determine the strength of inhibition, rate-level functions were plotted at the relevant ILD and then repeated for the same series of contralateral intensities in the absence of an ipsilateral stimulus. This procedure was done only for cases in which the presence of inhibition had been established through an inhibitory rate-intensity function. Inhibitory strength was defined as the proportion of area under the monaural (i.e., contralateral only) rate-level curve that was suppressed by ipsilateral sound. Inhibitory strength ranged from 0 (no inhibition) to 1 (complete inhibition). To illustrate the range of results, Fig. 7*A* shows data from neurons at maximum, median, and minimum inhibitory strength in both age groups. As is apparent in Fig. 7*A, middle*, the median inhibition strength was far greater in the juvenile than in the adult population. This observation implies that juvenile neurons received relatively strong inhibition compared with that of adult neurons. A direct comparison of the juvenile and adult population data (Fig. 7*B*) confirmed that they differ significantly ($P = 0.001$, Wilcoxon rank sum test). In addition, all cells tested in juvenile animals ($n = 17$) showed statistically significant inhibition, whereas inhibition achieved statistical significance in only 15 of 29 adult neurons analyzed; this difference between the age groups was significant ($P = 0.0006$, χ^2 analysis).

Theoretical implications for LSO coding

To consider how ipsilateral inhibition of MNTB neurons could influence the response of their postsynaptic target neurons in the LSO, we implemented a simple linear model of the LSO (see METHODS). The data suggested that strong inhibition occurred more frequently in juvenile MNTB neurons, and the model focuses on this age group. Figure 8 (*top*) shows the LSO response when it is activated by two monaural inputs, the AVCN and an uninhibited MNTB. The LSO neuron response over the stimulus space of intensity levels at the two ears is equal to the AVCN activity minus the MNTB activity. The unshaded portion of the LSO response surface represents physiological ILDs in the 3- to 5-kHz range (J. S. Green, M. N. Semple, and D. H. Sanes, unpublished observations), one of the most commonly tested ranges in juvenile animals in this study. In this region, LSO responses are relatively small. In contrast, adding inhibition of the MNTB to the model (*bottom*) results in greater LSO responsiveness within the region of physiological ILDs. Thus inhibition of the MNTB may enable juvenile LSO neurons to modulate their discharge rate to the relatively small physiological ILDs present at that age.

DISCUSSION

We found that about half of MNTB neurons in juvenile and adult gerbils were inhibited by sound stimuli at the ipsilateral ear. The inhibition affected prepotentials and postsynaptic action potentials equally, implying that inhibition was presynaptic to the MNTB neuron. Inhibitory thresholds did not differ by age and varied widely relative to excitatory thresholds. However, neurons in juvenile animals were, on average, more strongly inhibited than those recorded in adult animals. Previous studies of the MNTB have rarely described sound at the ipsilateral ear influencing responses in the MNTB (Goldberg and Brown 1968). This may reflect the fact that only half of adult MNTB neurons are inhibited, and many of these display weak inhibition that is obscured at high contralaterally evoked discharge rates. Thus the rarity of strong inhibition in adults, coupled with the fact that inhibition is most likely to be revealed by careful testing at near-threshold contralateral intensity levels, may account for differences between the present report and published findings. Alternatively, there may be differences between species.

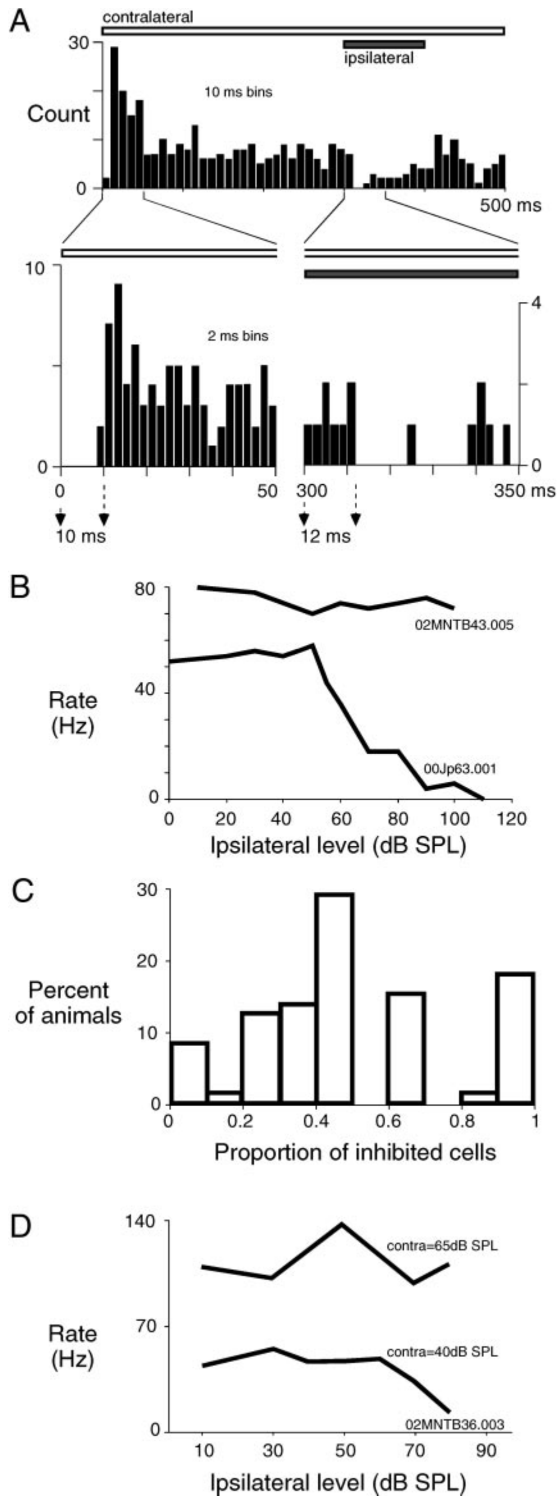

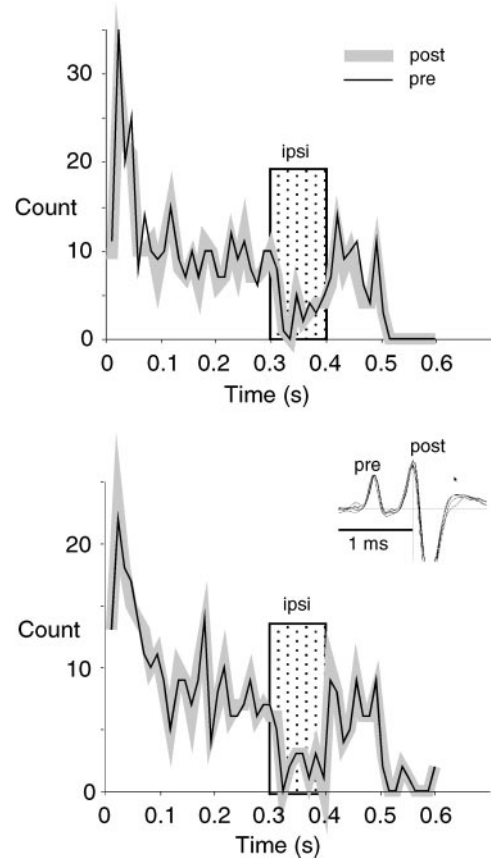

FIG. 5. Pre- and postsynaptic responses are inhibited by ipsilateral sound. Simultaneous measurements of pre- and postsynaptic action potentials are shown for 2 cells. Cells were activated for 500 ms by contralateral BF tones. For 100 ms, activity was inhibited by ipsilateral BF tones (▨). The effects of inhibition on pre- and post potentials were virtually identical. *Inset*: the waveform of the 2nd cell (*bottom*). All simultaneous pre- and postpotential recordings were made in adult animals.

Source of inhibition to the MNTB

We found that pre- and postsynaptic action potentials within the MNTB were inhibited equally by ipsilateral sound. There-

FIG. 4. Some MNTB neurons are inhibited by ipsilateral sound. *A*: latency of contralaterally evoked excitation and ipsilaterally evoked inhibition were similar. A 500-ms tone was presented to the contralateral ear and a 50-ms tone to the ipsilateral ear was delayed by 300 ms (*top*). As shown in the expanded portions of the historgram, the excitatory latency was 10 ms (*left*) and the inhibitory latency was 12 ms (*right*). *B*: plot shows the response of 2 MNTB neurons in response to ipsilateral best frequency (BF) tones at variety of intensity levels; to drive a baseline response, all ipsilateral tones were accompanied by BF contralateral tones of fixed intensity level. The top neuron displays no inhibition, while the bottom neuron is inhibited completely. Fifty percent of adult cells and 44% of juvenile cells were inhibited. *C*: inhibition is not restricted to particular animals. For cases in which ≥2 cells were tested for inhibition in the same animal, the proportion of cells inhibited was computed. The population results are shown as the black bars. Most animals had inhibited and noninhibited cells. *D*: increase in excitatory drive could obscure ipsilaterally evoked inhibition. Two rate-level plots are shown for a MNTB neuron. Top trace was obtained with a stronger contralateral stimulus (65 dB SPL) and displayed no inhibition as ipsilateral level was increased. The both trace was obtained with a weaker contralateral stimulus (40 dB SPL) and did display inhibition.

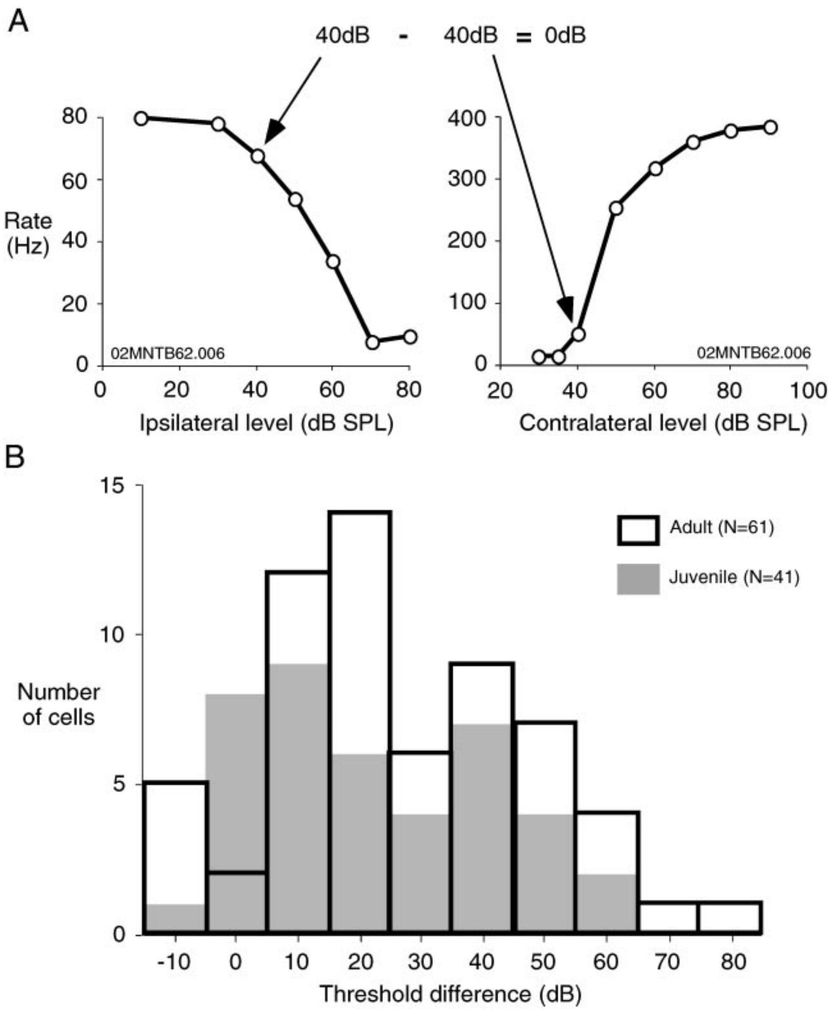

FIG. 6. Threshold differences between excitation and inhibition. *A*: calculation of threshold differences. The threshold of inhibition is obtained from the inhibitory rate-intensity function (*left*) in which ipsilateral instensity is varied while the cell is driven by a constant contralateral sound. The threshold of excitation is derived from the rate-intensity function (*right*) in which the intensity of the contralateral sound is varied. The threshold difference equals the inhibitory threshold minus the excitatory threshold. *B*: population data for threshold differences. Juvenile and adult cells have a wide range of threshold differences. Median threshold differences are 20 dB (adults) and 15 dB (juvenile). A Wilcoxon rank sum test revealed no significant difference between the group medians ($P = 0.33$).

fore inhibition must be presynaptic to the principal cells. Because electron microscopic studies have not revealed synapses on the calyces of Held (Smith et al. 1998), we conclude that ipsilateral inhibition is not acting within the MNTB. Alternative sources of inhibition include any inhibitory input to the cochlea or to the cochlear nucleus that provides excitatory afferent input to the MNTB.

One possible locus of inhibition is the cochlea because olivocochlear inputs can suppress cochlear activity in response to contralateral sound. However, this effect increases with age in gerbils, and no evidence of suppression was found at 22 days, the youngest age tested (Huang et al. 1994). Moreover, olivocochlear suppression requires ~100–200 ms to emerge (Warren and Liberman 1989), a much longer time scale than observed in the present study.

A second potential locus for inhibition is the globular bushy cells within the VCN. Each cochlear nucleus sends glycinergic projections to the opposite VCN, and both in vitro and in vivo recordings confirm that short-latency inhibition in the CN is elicited by contralateral stimulation (Babalian et al. 2002; Needham and Paolini 2003; Schofield and Cant 1996a,b; Shore et al. 2003; Wenthold 1987). In the rat cochlear nucleus, 30% of neurons are inhibited by contralateral stimuli, and the latency is only ~2 ms longer than ipsilateral excitation (Shore et al. 2003). Therefore this crossed inhibitory pathway provides the simplest explanation for the present results.

Several SOC and periolivary nuclei project to the VCN (Ostapoff et al. 1997; Schofield 1994; Shore et al. 1991), and these may provide alternative sources of inhibition. The ipsilateral MNTB, itself, projects to the VCN, and labeled presynaptic boutons appear to contact globular bushy cells (Schofield 1994). Therefore a projection from the MNTB to its ipsilateral cochlear nucleus could mediate inhibition by contralateral sound. Similarly, VNTB neurons can be excited by contralateral sound, and VNTB axons send a putative inhibitory projection to VCN (Goldberg and Brown 1968; Guinan et al. 1972; Ostapoff et al. 1997). Finally, descending inputs to the cochlear nucleus from the IC could also contribute to the present phenomenon, although these inputs are not thought to be inhibitory, do not contact the part of the nucleus that contains bushy cells (reviewed by Ostapoff et al. 1997) and would have produced longer inhibitory latencies than were observed in our recordings (Fig. 4*A*).

Implications for postsynaptic brain stem nuclei

Our findings suggest that, during juvenile development, the MNTB may exhibit distinct coding properties. As illustrated in Fig. 8, inhibition to the MNTB could permit LSO neurons to

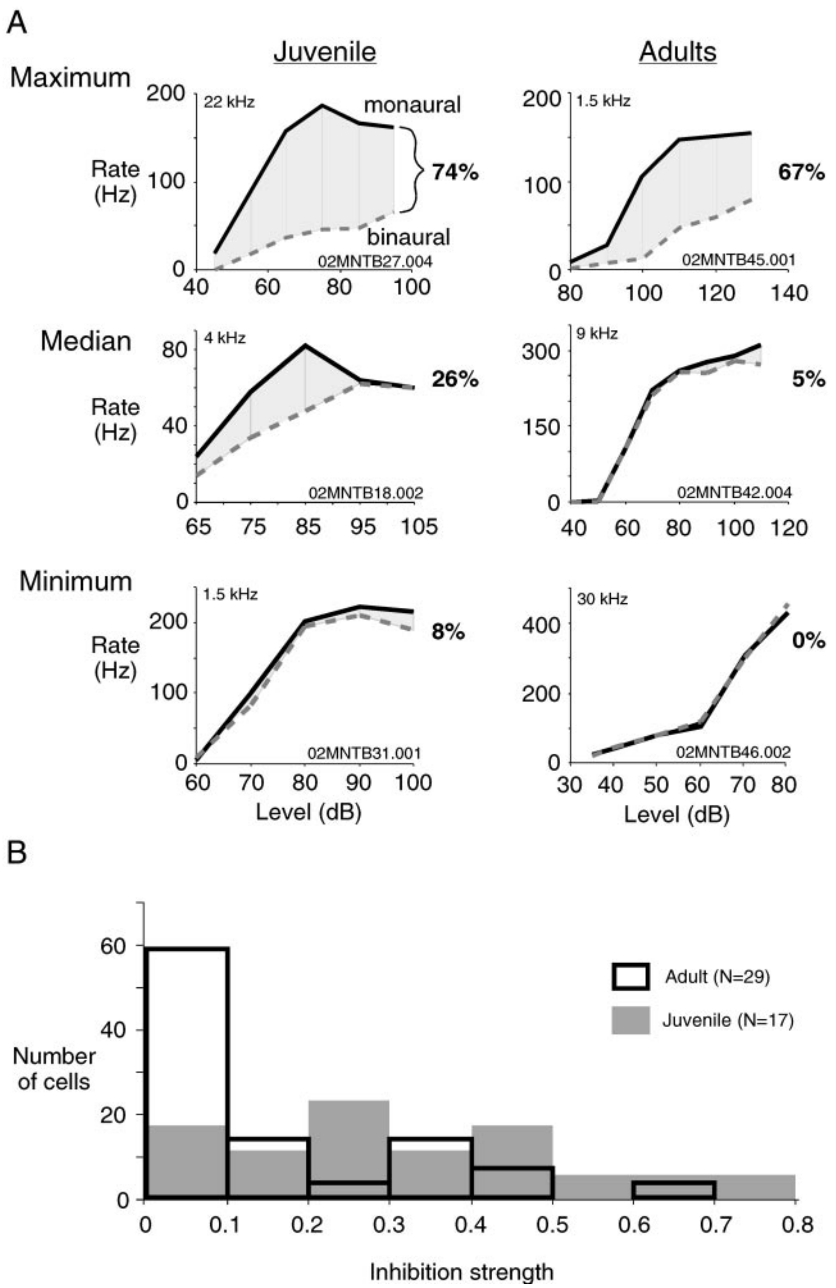

FIG. 7. Inhibition strengths in juvenile and adult animals. *A*: maximum, median, and minimum inhibition strengths in each age group. As an illustration of the method of computing inhibition strength, consider the *top left plot.* In this instance, binaural stimuli are presented at 0 ILD at varying intensities, and the response to these stimuli are shown (gray dashed line). Black line, what happens when the contralateral ear is stimulated as before but the ipsilateral ear receives no input. Thus the effect of ipsilateral sound is represented by the difference between the curves. The inhibition strength is the area between the curves as a percentage of the area under the monaural curve; in this case, it is 74%. In all cases, binaural stimuli were presented at 0 ILD. To distinguish true inhibition from random changes in discharge rate, monaural and binaural data were randomly reshuffled and the distribution of inhibition strengths expected by chance was derived from repeated reshuffling (see METHODS). From top to bottom in each column, are the maximum, median, and minimum inhibition strengths found in each population. For neurons in juvenile animals (n = 17), these strengths were 0.74, 0.26, and 0.08, whereas for adults (n = 29 cells) they were 0.67, 0.05, and 0. Comparison of the median plots suggests that cells in juvenile animals tend to be more strongly inhibited. *B*: full distributions in juvenile and adult animals. The adult distribution is biased toward weaker inhibition. The distributions are significantly different (P = 0.004, Kolmogorov-Smirnov test) as are their medians (P = 0.001, Wilcoxon rank-sum test).

respond to an acoustically relevant range of ILDs. In fact, inhibitory thresholds are relatively low in juvenile LSO neurons, particularly for those with lower characteristic frequencies, and discharge rate varies for level differences favoring the ipsilateral ear (Sanes and Rubel 1988). Thus without the ipsilateral inhibition to MNTB, the LSO neuron would respond poorly, or not at all, to most binaural stimuli. One qualification to the model-based conclusions is that, in the case of very proximal sound, ILDs may be much larger than normal (Brungart et al. 1999). Therefore the major effect of the inhibition on LSO could be to shift responsiveness into the frontal azimuthal field rather than to rescue the LSO from nonresponsiveness.

MNTB inhibitory projections also play an important role in ITD processing by the MSO (Brand et al. 2002). The inhibition shifts the discharge rate to vary with ITD values near the midline. Thus ipsilateral inhibition of the MNTB could adjust the degree to which tuning shifts of this sort occur. Because ITD sensitivity is also found in the LSO (Batra et al. 1997; Finlayson and Caspary 1991; Joris 1996; Joris and Yin 1995), similar implications may apply.

Additional MNTB projections include those to the superior paraolivary nucleus (SPN) and ventral nucleus of the lateral lemniscus (VNLL). Evidence suggests that the MNTB inhibits some SPN neurons in response to contralateral sound (Kulesza et al. 2003a). The inhibition of the MNTB may permit more discharge in SPN neurons during sound stimulation and weaken offset responses. If SPN neurons are involved in duration tuning by being offset responders (Kulesza et al. 2003b), then the developmental decrease in the strength of inhibition of the MNTB may be necessary for the expression of mature SPN responses. An important qualification to these possibilities is that the globular bushy cells that drive the

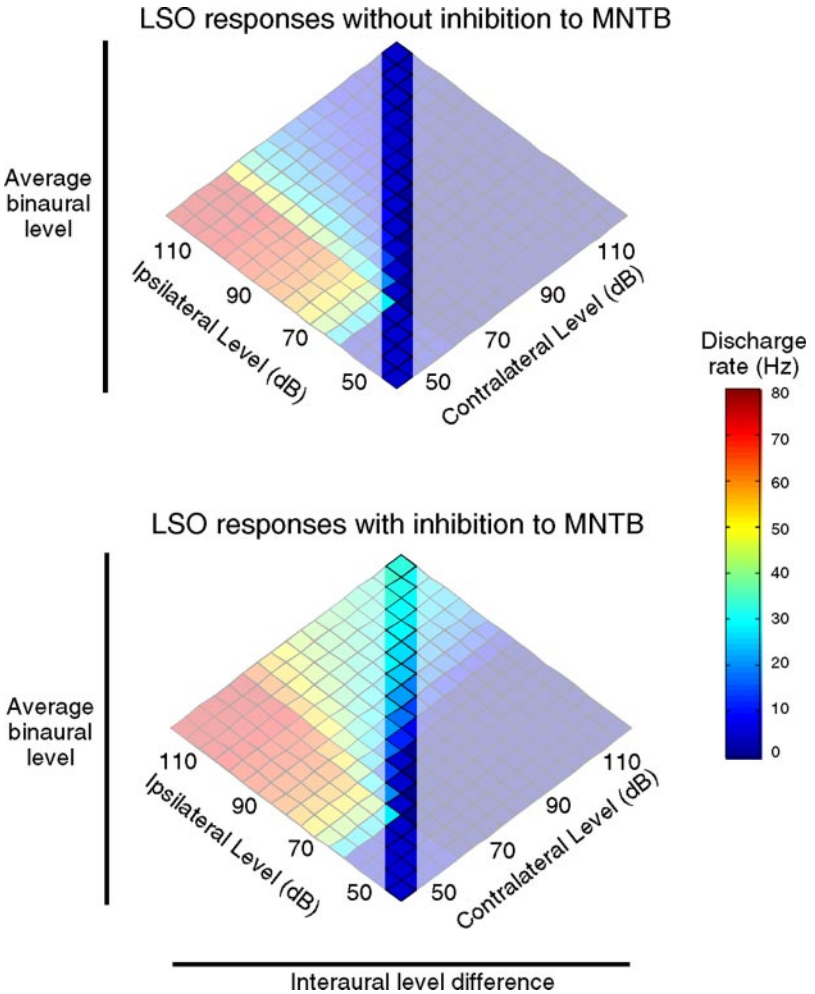

FIG. 8. Simple linear model of how LSO responses can be constructed from the activity of its inputs. *Top*: brain stem lacks inhibition of the MNTB. The ipsilateral intensity determines the amount of excitation as given in the AVCN response curve (see METHODS); the contralateral intensity sets the amount of inhibition, given in the MNTB response curve (see METHODS). The LSO discharge rate (color scale) is equal to the difference between AVCN-evoked excitation and MNTB-evoked inhibition and is shown as a function of ipsilateral and contralateral intensities. An alternative set of axes are ILD and average binaural level (ABL) axes. The transparent surfaces covering the LSO response surface define the boundary of physiologic and nonphysiologic ILDs. In the example, ILDs as large as 5 dB are within the uncovered area as would be appropriate for a juvenile animal at 3–5 kHz. *B*: inhibition of MNTB responses is added to the model. Inhibition to the LSO is therefore affected by contralateral and ipsilateral intensities. The model surface shows that the LSO is responsive further into the contralateral field than previously. The shaded portions of the surfaces have the same meaning as in the previous figure.

MNTB also project to SPN neurons (Cant and Benson 2003). Therefore inhibition of the globular bushy cells may produce opposing effects in the SPN by reducing direct excitation and releasing inhibition from the MNTB.

A minority of VNLL neurons are inhibited by contralateral stimulation and others have offset responses that may be due to release from inhibition (Batra and Fitzpatrick 1999). If inhibition from the MNTB is responsible for these effects, then ipsilateral inhibition of the MNTB would decrease the strength of the inhibition and offset responses in the VNLL. As with SPN, the supposition must be qualified by the observation that the VNLL receives a contralateral projection from globular bushy cells (Cant and Benson 2003) and opposing effects may therefore result from inhibition of the globular bushy cells.

Functional specializations during maturation

Functional specializations are found in the immature stages for species that undergo metamorphosis, often correlated with a dramatic change of habitat. For example, auditory midbrain neurons of the tadpole phase lock to AM frequencies ≤250 Hz, but the frequency range becomes quite restricted beginning at metamorphic climax (Boatright-Horowitz et al. 1997, 1999). In holometabolous insects, many neurons exhibit stage-specific properties (Tissot and Stocker 2000). For example, in the moth (*Manduca sexta*), a larval skeletal muscle motoneuron undergoes dramatic changes in dendritic arborization and electrical properties that accompany its de novo innervation of the adult cardiac chamber (Dulcis and Levine 2004).

The functional properties of developing neurons have often been shown to be inferior to those of adults. In the case of binaural processing, neurons from juvenile animals display limited dynamic ranges and irregular ILD functions as compared with adults (Moore and Irvine 1981; Sanes and Rubel 1988; Thornton et al. 1999). Limitations of auditory coding properties may be attributable, in part, to immature peripheral structures, such as the external ears. In the developing ferret, single auditory cortex neurons are not very directional but can respond in mature fashion when stimulated with sound cues that are only available to the adult due to the external ear filtering properties (Mrsic-Flogel et al. 2003). Gerbils clearly have the ability to localize species-specific vocalizations from a very early age, and the use of binaural cues is required (Kelly and Potash 1986). Therefore it is possible that their nervous system includes age-specific specializations that permit some minimum degree of performance given the constraints of small head and pinna size. In summary, the present results demonstrate that the MNTB, a major inhibitory projection nucleus in the auditory brain stem, is inhibited by stimuli to the ipsilateral ear. This result is observed in approximately half of the recorded neurons, and the strength of inhibition is far greater in neurons recorded from juvenile animals. MNTB target nuclei, such a LSO, which encode azimuthal sound location may, therefore perform these computations with the support of an additional brain stem circuit during juvenile development. The age-specific functional properties of MNTB neurons would permit responsiveness to small level differences that would otherwise go undetected.

ACKNOWLEDGMENTS

We thank M. Semple, L. Kiorpes, S. Kuwada, A. Reyes, and V. Kotak for insightful comments on earlier drafts of this manuscript.

GRANTS

This work was supported by National Institute of Deafness and Other Communications Disorders Grants DC-00540 and DC-05268.

REFERENCES

Babalian AL, Jacomme AV, Doucet JR, Ryugo DK, and Rouiller EM. Commissural glycinergic inhibition of bushy and stellate cells in the anteroventral cochlear nucleus. *Neuroreport* 13: 555–558, 2002.

Batra R and Fitzpatrick DC. Discharge patterns of neurons in the ventral nucleus of the lateral lemniscus of the unanesthetized rabbit. *J Neurophysiol* 82: 1097–1113, 1999.

Batra R, Kuwada S, and Fitzpatrick DC. Sensitivity to interaural temporal disparities of low- and high-frequency neurons in the superior olivary complex. I. Heterogeneity of responses. *J Neurophysiol* 78: 1222–1236, 1997. *Natl Acad Sci USA* 94: 14877–14882, 1997.

Boatright-Horowitz SS, Garabedian CE, Odabashian KH, and Simmons AM. Coding of amplitude modulation in the auditory midbrain of the bullfrog (*Rana catesbeiana*) across metamorphosis. *J Comp Physiol [A]* 184: 219–231, 1999.

Boatright-Horowitz SS and Simmons AM. Transient "deafness" accompanies auditory development during metamorphosis from tadpole to frog. *Proc Natl Acad Sci USA* 94: 14877–14882, 1997.

Boudreau JC and Tsuchitani C. Binaural interaction in the cat superior olive S segment. *J Neurophysiol* 31: 442–454, 1968.

Brand A, Behrend O, Marquardt T, McAlpine D, and Grothe B. Precise inhibition is essential for microsecond interaural time difference coding. *Nature* 417: 543–547, 2002.

Brungart DS, Durlach NI, and Rabinowitz WM. Auditory localization of nearby sources. II. Localization of a broadband source. *J Acoust Soc Am* 106: 1956–1968, 1999.

Cant NB and Benson CG. Parallel auditory pathways: projection patterns of the different neuronal populations in the dorsal and ventral cochlear nuclei. *Brain Res Bull* 60: 457–474, 2003.

Cant NB and Gaston KC. Pathways connecting the right and left cochlear nuclei. *J Comp Neurol* 212: 313–326, 1982.

Dulcis D and Levine RB. Remodeling of a larval skeletal muscle motoneuron to drive the posterior cardiac pacemaker in the adult moth, *Manduca sexta. J Comp Neurol* 478: 126–142, 2004.

Finlayson PG and Caspary DM. Low-frequency neurons in the lateral superior olive exhibit phase-sensitive binaural inhibition. *J Neurophysiol* 65: 598–605, 1991.

Friauf E and Ostwald J. Divergent projections of physiologically characterized rat ventral cochlear nucleus neurons as shown by intra-axonal injection of horseradish peroxidase. *Exp Brain Res* 73: 263–284, 1988.

Galambos R, Schwartzkopff J, and Rupert A. Microelectrode study of superior olivary nuclei. *Am J Physiol* 197: 527–536, 1959.

Goldberg JM and Brown PB. Functional organization of the dog superior olivary complex: an anatomical and electrophysiological study. *J Neurophysiol* 31: 639–656, 1968.

Goldberg JM and Brown PB. Response of binaural neurons of dog superior olivary complex to dichotic tonal stimuli: some physiological mechanisms of sound localization. *J Neurophysiol* 32: 613–636, 1969.

Grothe B and Sanes DH. Bilateral inhibition by glycinergic afferents in the medial superior olive. *J Neurophysiol* 69: 1192–1196, 1993.

Guinan JJJ and Li RY. Signal processing in brainstem auditory neurons which receive giant endings (calyces of Held) in the medial nucleus of the trapezoid body of the cat. *Hear Res* 49: 321–334, 1990.

Guinan Jr JJ, Norris BE, and Guinan SS. Single auditory units in superior olivary complex. II. Locations of unit categories and tonotopic organization. *Int J Neurosci* 4: 147–166, 1972.

Held H. Die centrale Gehörleitung. *Arch Anat Physiol Anat Abteil* 17: 201–248, 1893.

Henkel CK and Brunso-Bechtold JK. Dendritic morphology and development in the ferret lateral superior olivary nucleus. *J Comp Neurol* 313: 259–272, 1991.

Huang JM, Berlin CI, Cullen JK, and Wickremasinghe AR. Development of contralateral suppression of the VIIIth nerve compound action potential (CAP) in the Mongolian gerbil. *Hear Res* 78: 243–248, 1994.

Joshi I and Wang LY. Developmental profiles of glutamate receptors and synaptic transmission at a single synapse in the mouse auditory brain stem. *J Physiol* 540: 861–873, 2002.

Joris PX. Envelope coding in the lateral superior olive. II. Characteristic delays and comparison with responses in the medial superior olive. *J Neurophysiol* 76: 2137–2156, 1996.

Joris PX and Yin TC. Envelope coding in the lateral superior olive. I. Sensitivity to interaural time differences. *J Neurophysiol* 73: 1043–1062, 1995.

Kandler K and Friauf E. Development of glycinergic and glutamatergic synaptic transmission in the auditory brain stem of perinatal rats. *J Neurosci* 15: 6890–6904, 1995a.

Kandler K and Friauf E Development of electrical membrane properties and discharge characteristics of superior olivary complex neurons in fetal and postnatal rats. *Eur J Neurosci* 7: 1773–1790, 1995b.

Kapfer C, Seidl AH, Schweizer H, and Grothe B. Experience-dependent refinement of inhibitory inputs to auditory coincidence-detector neurons. *Nat Neurosci* 5: 247–253, 2002.

Kavanagh GL and Kelly JB. Midline and lateral field sound localization in the ferret (*Mustela putorius*): contribution of the superior olivary complex. *J Neurophysiol* 67: 1643–1658, 1992.

Kelly JB and Potash M. Directional responses to sounds in young gerbils (*Meriones unguiculatus*). *J Comp Psychol* 100: 37–45, 1986.

Kil J, Kageyama GH, Semple MN, and Kitzes LM. Development of ventral cochlear nucleus projections to the superior olivary complex in gerbil. *J Comp Neurol* 353: 317–340, 1995.

Kim G and Kandler K. Elimination and strengthening of glycinergic/GABAergic connections during tonotopic map formation. *Nat Neurosci* 6: 282–290, 2003.

Kopp-Scheinpflug C, Lippe WR, Dorrscheidt GJ, and Rubsamen R. The medial nucleus of the trapezoid body in the gerbil is more than a relay: comparison of pre- and postsynaptic activity. *J Assoc Res Otolaryngol* 4: 1–23, 2003.

Korada S and Schwartz IR. Development of GABA, glycine, and their receptors in the auditory brain stem of gerbil: a light and electron microscopic study. *J Comp Neurol* 12: 664–681, 1999.

Kotak VC, Korada S, Schwartz IR, and Sanes DH. A developmental shift from GABAergic to glycinergic transmission in the central auditory system. *J Neurosci* 18: 4646–4655, 1998.

Kulesza RJ, Spirou GA, and Berrebi AS Selective Effects of GABA and glycine on the response properties of neurons in the superior paraolivary nucleus of the rat. *Assoc Res Otolaryngol Abstr* 102, 2003a.

Kulesza RJ Jr, Spirou GA, and Berrebi AS. Physiological response properties of neurons in the superior paraolivary nucleus of the rat. *J Neurophysiol* 89: 2299–2312, 2003b.

Kuwabara N, DiCaprio RA, and Zook JM. Afferents to the medial nucleus of the trapezoid body and their collateral projections. *J Comp Neurol* 314: 684–706, 1991.

Kuwabara N and Zook JM. Projections to the medial superior olive from the medial and lateral nuclei of the trapezoid body in rodents and bats. *J Comp Neurol* 324: 522–538, 1992.

Masterton B, Jane JA, and Diamond IT. Role of brainstem auditory structures in sound localization. I. Trapezoid body, superior olive, and lateral lemniscus. *J Neurophysiol* 30: 341–359, 1967.

Mogdans J and Knudsen EI. Site of auditory plasticity in the brain stem (VLVp) of the owl revealed by early monaural occlusion. *J Neurophysiol* 72: 2875–2891, 1994.

Moore DR and Irvine DR. Development of responses to acoustic interaural intensity differences in the cat inferior colliculus. *Exp Brain Res* 41: 301–309, 1981.

Morest DK. The collateral system of the medial nucleus of the trapezoid body of the cat, its neuronal architecture and relation to the olivo-cochlear bundle. *Brain Res* 9: 288–311, 1968.

Mrsic-Flogel TD, Schnupp JW, and King AJ. Acoustic factors govern developmental sharpening of spatial tuning in the auditory cortex. *Nat Neurosci* 6: 981–988, 2003.

Needham K and Paolini AG. Fast inhibition underlies the transmission of auditory information between cochlear nuclei. *J Neurosci* 23: 6357–6361, 2003.

Ostapoff EM, Benson CG, and Saint Marie RL. GABA- and glycine-immunoreactive projections from the superior olivary complex to the cochlear nucleus in guinea pig. *J Comp Neurol* 381: 500–512, 1997.

Rietzel H-J and Friauf E. Neuron types in the rat lateral superior olive and developmental changes in the complexity of their dendritic arbors. *J Comp Neurol* 390: 20–40, 1998.

Russell FA and Moore DR. Afferent reorganisation within the superior olivary complex of the gerbil: development and induction by neonatal, unilateral cochlear removal. *J Comp Neurol* 352: 607–625, 1995.

Sanes DH. The development of synaptic function and integration in the central auditory system. *J Neurosci* 13: 2627–2637, 1993.

Sanes DH and Constantine-Paton M. The development of stimulus following in the cochlear nerve and inferior colliculus of the mouse. *Dev Brain Res* 22: 255–268, 1985.

Sanes DH, Malone BL, and Semple MN. Modulation of binaural level stimuli in gerbil inferior colliculus: role of synaptic inhibition. *J Neurosci* 18: 794–803, 1998.

Sanes DH and Rubel EW. The ontogeny of inhibition and excitation in the gerbil lateral superior olive. *J Neurosci* 8: 682–700, 1988.

Sanes DH and Siverls V. Development and specificity of inhibitory terminal arborizations in the central nervous system. *J Neurobiol* 8: 837–854, 1991.

Sanes DH, Song J, and Tyson J. Refinement of dendritic arbors along the tonotopic axis of the gerbil lateral superior olive. *Dev Brain Res* 67: 47–55, 1992.

Schofield BR. Projections to the cochlear nuclei from principal cells in the medial nucleus of the trapezoid body in guinea pigs. *J Comp Neurol* 344: 83–100, 1994.

Schofield BR and Cant NB. Origins and targets of commissural connections between the cochlear nuclei in guinea pigs. *J Comp Neurol* 375: 128–146, 1996a.

Schofield BR and Cant NB. Projections from the ventral cochlear nucleus to the inferior colliculus and the contralateral cochlear nucleus in guinea pigs. *Hear Res* 102: 1–14, 1996b.

Shore SF, Godfrey DA, Helfert RH, Altschuler RA, and Bledsoe SC. Connections between the cochlear nuclei in guinea pig. *Hear Res* 62: 16–26, 1992.

Shore SE, Helfert RH, Bledsoe SC, Altschuler RA, and Godfrey DA. Descending projections to the dorsal and ventral divisions of the cochlear nucleus in guinea pig. *Hear Res* 52: 255–268, 1991.

Shore SE, Sumner CJ, Bledsoe SC, and Lu J. Effects of contralateral sound stimulation on unit activity of ventral cochlear nucleus neurons. *Exp Brain Res* 153: 427–435, 2003.

Smith PH, Joris PX, and Yin TC. Anatomy and physiology of principal cells of the medial nucleus of the trapezoid body (MNTB) of the cat. *J Neurophysiol* 79: 3127–3142, 1998.

Sommer I, Lingenhöhl K, and Friauf E. Principal cells of the rat medial nucleus of the trapezoid body: an intracellular in vivo study of their physiology and morphology. *Exp Brain Res* 95: 223–239, 1993.

Spitzer MW and Semple MN. Neurons sensitive to interaural phase disparity in gerbil superior olive: diverse monaural and temporal response properties. *J Neurophysiol* 73: 1668–1690, 1995.

Svirskis G, Kotak VC, Sanes DH, and Rinzel J. Sodium along with low threshold potassium currents enhance coincidence detection of subthreshold noisy signals in MSO neurons. *J Neurophysiol* 91: 2465–2473, 2004.

Thornton SK, Semple MN, and Sanes DH. Conditioned enhancement and suppression in the developing auditory midbrain. *Eur J Neurosci* 11: 1414–1420, 1999.

Tissot M and Stocker RF. Metamorphosis in Drosophila and other insects: the fate of neurons throughout the stages. *Prog Neurobiol* 62: 89–111, 2000.

Warren EH and Liberman MC. Effects of contralateral sound on auditory-nerve responses. I. Contributions of cochlear efferents. *Hear Res* 37: 89–104, 1989.

Wenner P and O'Donovan MJ. Mechanisms that initiate spontaneous network activity in the developing chick spinal cord. *J Neurophysiol* 86: 1481–198, 2001.

Wenthold RJ. Evidence for a glycinergic pathway connecting the two cochlear nuclei: an immunocytochemical and retrograde transport study. *Brain Res* 415: 183–187, 1987.

Winmill RE and Hedrick MS. Developmental changes in the modulation of respiratory rhythm generation by extracellular K^+ in the isolated bullfrog brainstem. *J Neurobiol* 55: 278–287, 2003.

Wu SH and Kelly JB. Physiological evidence for ipsilateral inhibition in the lateral superior olive: synaptic responses in mouse brain slice. *Hear Res* 73: 57–64, 1994.

Yin TC and Chan JC. Interaural time sensitivity in medial superior olive of cat. *J Neurophysiol* 64: 465–488, 1990.